



## Amide-based derivatives of $\beta$ -alanine hydroxamic acid as histone deacetylase inhibitors: Attenuation of potency through resonance effects

Vivian Liao<sup>a</sup>, Tao Liu<sup>b</sup>, Rachel Codd<sup>a,\*</sup>

<sup>a</sup> School of Medical Sciences (Pharmacology) and Bosch Institute, University of Sydney, New South Wales 2006, Australia

<sup>b</sup> Children's Cancer Institute Australia, Sydney Children's Hospital, New South Wales 2031, Australia

### ARTICLE INFO

#### Article history:

Received 13 June 2012

Revised 23 July 2012

Accepted 1 August 2012

Available online 9 August 2012

#### Keywords:

Histone deacetylase inhibitors  
Trichostatin A

### ABSTRACT

A library of amide-linked derivatives of  $\beta$ -alanine hydroxamic acid were prepared (**2–7**) and the activity as inhibitors of Zn(II)-containing histone deacetylases (HDACs) determined in vitro against HDAC1 and the anti-proliferative activity determined in BE(2)-C neuroblastoma cells. The IC<sub>50</sub> values of the best-performing compounds (**3–7**) against HDAC1 ranged between 38 and 84  $\mu$ M. The least potent compound (**2**) inhibited a maximum of only 40% HDAC1 activity at 250  $\mu$ M. The anti-proliferative activity of **2–7** at 50  $\mu$ M against BE(2)-C neuroblastoma cells ranged between 57.0% and 88.6%. The structural similarity between the potent HDAC inhibitor trichostatin A (TSA, **1**; HDAC1, IC<sub>50</sub> 12 nM) and the present compounds (**2–7**) was high at the Zn(II) coordinating hydroxamic acid head group; and in selected compounds (**2**, **5**), at the 4-(dimethylamino)phenyl tail. The significantly reduced potency of **2–7** relative to **1** underscores the rank importance of the linker region as part of the HDAC inhibitor pharmacophore. Molecular modeling of **1–7** using HDAC8 as the template suggested that the conformationally constrained 4'-methyl group of **1** may contribute to HDAC inhibitor potency through a sandwich-like interaction with a hydrophobic region containing F152 and F208; and that the absence of this group in **2–7** may reduce potency. The close proximity of the 5'-carbonyl oxygen atom in **2–7** to the sulfur atom of Met274 in HDAC8 or the corresponding isobutyl group of Leu274 in HDAC1 may attenuate potency through repulsive steric and dipole–dipole forces. In a unique resonance stabilized form of **2**, this interaction could manifest as stronger ion-dipole repulsive forces, resulting in a further decrease in potency. This work suggests that resonance structures of HDAC inhibitors could modulate intermolecular interactions with HDAC targets, and potency.

© 2012 Elsevier Ltd. All rights reserved.

Some of the most potent inhibitors of Class I/II and IV of the histone deacetylases (HDACs), which are targets at the forefront of cancer research, contain a hydroxamic acid group that inactivates the Zn(II) ion at the HDAC active site. In concert with histone acetyltransferases, HDACs modulate the acetylation status of the  $\epsilon$ -amino group of surface-exposed lysine residues in nucleosomal histones, which affects chromatin topology and transcriptional activity. Hypo-acetylated histones that result from upregulated HDAC activity or downregulated histone acetyltransferase activity increase the relative concentration of condensed chromatin which represses the transcription of tumor suppressor genes and promotes the onset and progression of tumors.<sup>1–3</sup> The metal coordinating ability of the hydroxamic acid functional group has broad utility in clinical settings,<sup>4,5</sup> with hydroxamic acid-based HDAC inhibitors such as suberoylanilide hydroxamic acid (SAHA or

vorinostat; HDAC1, IC<sub>50</sub> 48 nM) for the treatment of cutaneous T-cell lymphoma, a notable example.<sup>3,6</sup> Even more potent than SAHA, is the natural hydroxamic acid trichostatin A (2E,4E,6R)-7-[4-(dimethylamino)phenyl]-N-hydroxy-4,6-dimethyl-7-oxohepta-2,4-dienamide (**1**) produced by *Streptomyces platensis*, *Streptomyces hygroscopicus* Y-50 or *Streptomyces sioyaensis* (HDAC1, IC<sub>50</sub> 12 nM).<sup>7,8</sup> This compound is costly to access from culture and is difficult to synthesize,<sup>9</sup> which calls for the design of analogues of **1** as potential HDAC inhibitors.

The pharmacophore of hydroxamic acid-based HDAC inhibitors has been defined as comprising three elements: a Zn(II) coordinating hydroxamic acid group, a terminal aromatic group, and a linker region.<sup>10–12</sup> In order to better understand the contribution of the linker region to the pharmacophore, we prepared a library of amide-linked derivatives of  $\beta$ -alanine hydroxamic acid, some candidates which shared with **1**, the first two elements of the pharmacophore.

Amide-linked precursors were prepared from the HOBt-based, EDC-activated conjugation of *para*-substituted (X = dimethylamino, methyl, nitro, H) derivatives of cinnamic acid, 3-phenylpropanoic

Abbreviations: HDAC, histone deacetylase; TSA, trichostatin A; SAHA, suberoylanilide hydroxamic acid.

\* Corresponding author. Tel.: +61 (0)2 9351 6738; fax: +61 (0)2 9351 4717.

E-mail address: [rachel.codd@sydney.edu.au](mailto:rachel.codd@sydney.edu.au) (R. Codd).

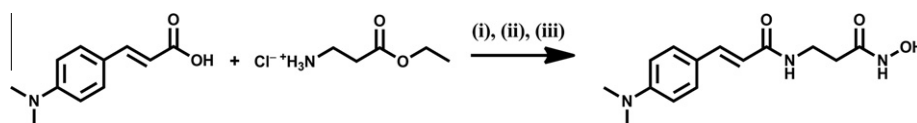
acid, 2-phenylacetic acid or 2-phenoxyacetic acid; and  $\beta$ -alanine ethyl ester hydrochloride. Following hydrolysis of the ethyl ester, the hydroxamic acid group was installed from the reaction between the mixed anhydride formed in situ from chloroethylformate and *N*-methylmorpholine; and hydroxylamine (Scheme 1). After work-up, when sprayed with an ethanol solution of Fe(III), the final spot of the product on a TLC plate turned pale pink, as evidence of the metal-coordinating ability of the hydroxamic acid group. The products (Table 1) were characterised by  $^1\text{H}$  and  $^{13}\text{C}$  NMR spectroscopy, ESI-MS and microanalysis (Supplementary data). Relative to the free carboxylic acid, the signals in the  $^1\text{H}$  NMR spectra assigned to the  $\alpha$ -methylene protons shifted upfield by about 0.2 ppm in the corresponding hydroxamic acid.

The  $\text{IC}_{50}$  values of 2–7 against HDAC1 were determined using a fluorometric assay and the anti-proliferative effects of the compounds were determined against BE(2)-C neuroblastoma cells using the Alamar blue assay (Fig. 1, Table 1).<sup>13–15</sup> Compared to the  $\text{IC}_{50}$  value of 1 against HDAC1 ( $\text{IC}_{50}$  12 nM), 2–7 had significantly decreased potency (38–84  $\mu\text{M}$ ). Compound 2 inhibited only a maximum of 40% HDAC1 activity at 250  $\mu\text{M}$ , and was the least potent compound. The  $\text{IC}_{50}$  value of SAHA against HDAC1 determined in the current work ( $110.8 \pm 1.1$  nM) calibrated the results to literature  $\text{IC}_{50}$  values for SAHA;<sup>16</sup> and supported the veracity of the data for 2–7. Given the similarity between 2–7 and 1, with respect to the Zn(II) coordinating hydroxamic acid group; and between 2, 5 and 1, with respect to the 4-(dimethylamino)phenyl group, the low potency against HDAC1 was unexpected. Most surprising was the extraordinarily low potency of 2 against HDAC1. The whole cell-based assay system gave an activity profile that differed from the profile established using isolated HDAC1. At 50  $\mu\text{M}$  the anti-proliferative activity of 2–7 against BE(2)-C neuroblastoma cells ranged between 57.0 and 88.6%, with 2 the most potent compound. Other work has shown differences between the activities of compounds screened using isolated HDACs or whole-cell assay systems, with belinostat and SAHA a notable example (belinostat:SAHA; biochemical activity ( $\sim 1:1$ ), anti-proliferative activity against a selection of cancer cell lines ( $\sim 1.7\text{--}7:1$ )).<sup>17</sup> This is likely due to the higher complexity of the whole cell-based assay system with regard to the involvement of HDACs in regulating the acetylation of non-histone proteins ( $\alpha$ -tubulin, tumor suppressor p53) and the optimal activity of most HDACs requiring the formation of multiprotein complexes. The  $\text{IC}_{70}$  values of 1 or SAHA were determined in BE(2)-C neuroblastoma cells as 0.05  $\mu\text{M}$  or 2  $\mu\text{M}$ , respectively. Compound 7 has been reported to inhibit 19% of HDAC activity in HeLa extract at 1  $\mu\text{M}$ , but was not further developed as a lead.<sup>18</sup>

Molecular modelling (HyperChem 7.5, MM+ force field for energy minimization) was used to inform the  $\text{IC}_{50}$  results of 2–7 against HDAC1. Three X-ray crystal structures of human HDACs with 1<sup>19,20</sup> and one structure of a prokaryotic HDAC homologue with 1 have been solved.<sup>21</sup> The X-ray crystal structure of 1 bound to human HDAC8<sup>19</sup> was used as the template. The coordinate bonds between 1 and Zn(II) were deleted and the isolated fragment was used to build models of each of 2–7 with zero charge. The protein and the hydroxamic acid group (C(O)NH(OH)) of the model of 2–7 were frozen and the remaining structure of the free ligand was minimized. At the completion of the minimization process, the

coordinate bonds between the hydroxamic acid group and the Zn(II) ion were re-installed. This method assumes that the bidentate hydroxamate coordination between 2 and 7 and Zn(II) will not differ significantly from the 1-Zn(II) coordination observed in the X-ray crystal structure. The method allows for the structure of 2–7 distal to the active site Zn(II) to be optimized within the constraints of the HDAC8 active site cavity. The veracity of the method was supported by the close agreement between the conformation of native 1 and 1 which was minimized within the HDAC8 active site as described for 2–7 (Fig. 2, far left). The overlaid structures of minimized 1 and each of 2–7 are shown in Figure 2. Despite the variation in the number of main-chain atoms in the linker separating the hydroxamic acid head group from the phenyl-substituted tail (six atoms: 2–4, 7; five atoms: 5, 6), the phenyl group in most cases minimized to a position that coalesced closely with the phenyl group of 1. The poorest overlay of phenyl groups occurred between 1 and 4 (Fig. 2, middle). In this case, the ethylene group proximal to the tolyl group was sufficiently flexible to mine a local hydrophobic pocket in the protein, which re-directed the orientation of the tolyl group. This local conformational flexibility was not available to other candidates, due to unsaturation (2, 7), an insufficient number of methylene groups (5, 6) or the presence of a methoxy group subject to electron delocalization effects (3).

The linker region of 1 is more complex than 2–7, with two methyl substituents, one chiral carbon (6*R*) and two unsaturated carbon–carbon bonds (2*E*, 4*E*). In the X-ray crystal structure of 1 bound to HDAC8, the 4'-methyl group is positioned in a sandwich-like fashion between the aromatic rings of F152 and F208 with the distance from each plane of the aromatic ring to the methyl group carbon atom equal at 3.84 Å (Fig. 3). This hydrophobic interaction was not available to 2–7 (Fig. 3, shown for 2) and may be a factor that contributed to their low potency as HDAC1 inhibitors. The structures of 2–7 as minimized in the HDAC8 active site cavity revealed a close distance between the 5'-carbonyl oxygen atom and the sulfur atom of Met274. In 2 and 7, this distance was 3.5 Å, which is close to the sum of the sulfur and oxygen van der Waals radii (3.3 Å)<sup>22</sup> and raises the possibility of the carbonyl oxygen atom-mediated oxidation of the Met274 sulfur atom in HDAC8, as shown to occur in amyloid  $\beta$ -peptide.<sup>23,24</sup> Inhibitor potency was determined against HDAC1, which instead of the four amino acid sequence P273-M274-C275-S276 in HDAC8, contains R273-L274-G275-C276.<sup>25</sup> In silico mutation of PMCS(HDAC8)  $\rightarrow$  RLGC(HDAC1) followed by minimization of 2–7 and RLGC only, with the remaining protein constrained, showed that the 5'-carboxyl oxygen atom of 2 was in close proximity to the isobutyl side chain of Leu274, with one oxygen–hydrogen (methyl) distance of 2.8 Å. It is proposed that the proximity of the 5'-carbonyl oxygen atom in 2–7 to Leu274 in HDAC1 is a contributing factor to the low potency of this group of compounds. Reduced binding to the active site would arise from steric repulsion and from repulsive dipole–dipole interactions, since the molecular dipole in leucine is orientated from the  $\alpha$ -carbon atom (positive) along the isobutyl tail (negative). Due to the presence of the electron donating dimethylamino substituent ( $\sigma_p$  -0.83) in 2 and the conjugated linker region, this compound could comprise different contributing resonance structures (Fig. 4a). In the



**Scheme 1.** Synthesis of amide-linked derivatives of  $\beta$ -alanine hydroxamic acid: reagents and conditions (shown for 2). (i) HOBt, EDC-HCl, DIPEA, DMF, RT, 16 h; (ii) NaOH, MeOH, RT, 30 min; (iii) EtOCOCl, NMM,  $\text{NH}_2\text{OH}$ , MeOH, RT, 15 min.

**Table 1**  
Synthesis and activity measurements of **2–7**

	Structure	Activity	
		IC <sub>50</sub> HDAC1 <sup>a</sup> (μM)	Neuroblastoma cells <sup>b</sup> (%)
1		0.012	c
2		>250 <sup>d</sup>	57.0 (1.1)
3		84.0 (4.6)	80.4 (1.8)
4		80.0 (1.5)	72.4 (1.7)
5		38.0 (1.9)	62.8 (2.4)
6		39.4 (0.3)	87.9 (3.8)
7		67.0 (6.7)	88.6 (1.6)

<sup>a</sup> Results reported as an average of  $n = 3$  with standard error of the mean in brackets.

<sup>b</sup> Results from a concentration of 50 μM reported as an average of  $n = 9$  with standard error of the mean in brackets.

<sup>c</sup> The IC<sub>70</sub> values of TSA or SAHA were determined in BE(2)-C neuroblastoma cells as 0.05 μM or 2 μM, respectively.

<sup>d</sup> Maximal inhibition of HDAC1 of 40% at 250 μM.

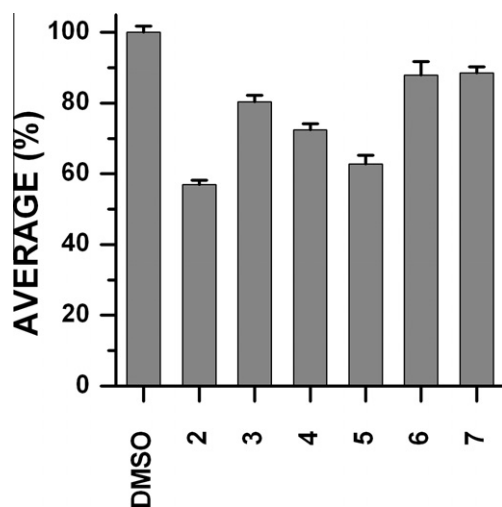


**Figure 1.** Anti-proliferative activity of **2–7** against BE(2)-C neuroblastoma cells.

resonance structure of **2** which features a negative charge on the 5'-carboxyl oxygen atom, the intermolecular repulsive force with Leu274 (HDAC1) or Met274 (HDAC8) would increase in strength from a dipole–dipole force (**3–7**) (Fig. 4b, shown for **7**, in which

the dimethylamino group is absent) to an ion-dipole force (**2**). This provides a rationale that accommodates for both the low potency of **2–7** as a group relative to **1**; and the extraordinarily low potency of **2**, relative to **3–7**. The distance between the 7'-carbonyl oxygen atom of **1** which could exist in two resonance forms and atoms of the corresponding side chains (Met274, Leu274) is sufficient to reduce these intermolecular repulsions (Fig. 4c). In summary, the absence of the 4'-methyl group in **2–7** prevents favorable van der Waals binding effects with F152 and F208, as posited for **1**. As a group, there may be additional reductions in HDAC inhibitor potency in **2–7** due to repulsive steric and dipole–dipole effects resulting from the close proximity of the 5'-carbonyl oxygen atom and the isobutyl group of Leu274 (HDAC1) or the sulfur atom in Met274 (HDAC8). The existence of unique resonance stabilized forms of **2** could manifest as further decreases in potency, due to the increased repulsive ion-dipole force between the anionic 5'-carbonyl oxygen atom and these residues. The work has demonstrated that the positioning of the amide bond in the linker region of HDAC inhibitors has a significant effect on potency and that resonance stabilized structures of compounds should be factored into the drug design process. In this case, the resonance stabilization appears to have attenuated potency. It remains conceivable that this effect could be used to positively modulate potency in HDAC inhibitors.

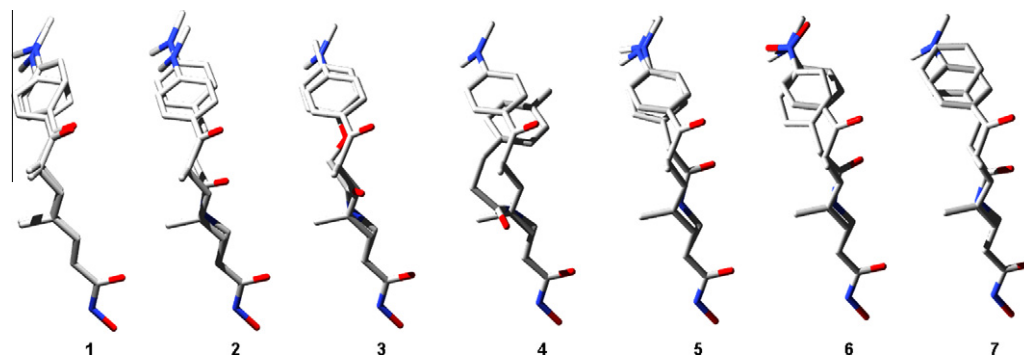


**Figure 2.** The overlay of **1** as from the X-ray crystal structure of **1**-bound HDAC8,<sup>19</sup> and **1** as minimized in the HDAC8 active site. The models of **2–7** as minimized within the HDAC8 active site are overlaid with the model of **1**. Excluding the atoms comprising the hydroxamic acid group ( $-\text{C}(\text{O})\text{NHOH}$ ), the compounds were minimized in the presence of the static HDAC8 enzyme. Hydrogen atoms have been omitted for clarity.

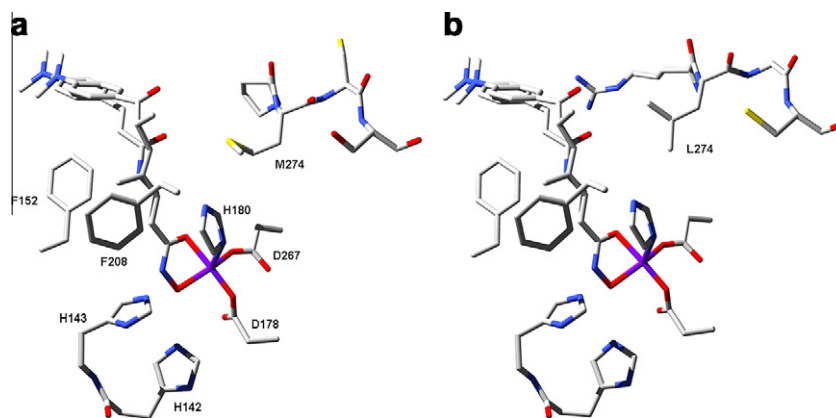


**Figure 3.** Overlaid structures of minimized models of **1** or **2** bound to the active site of HDAC8 (a) or HDAC1 (as generated by in silico mutation of HDAC8) (b). Apart from PMCS (HDAC8) and RLG (HDAC1), the residues located within 5 Å of the Zn(II) ion are conserved between HDAC8 and HDAC1. The close distance between the 5'-carbonyl oxygen atom in **2–7** and the sulfur atom in Met274 (HDAC8) or the isobutyl group of Leu274 (HDAC1) may attenuate HDAC inhibitor potency.

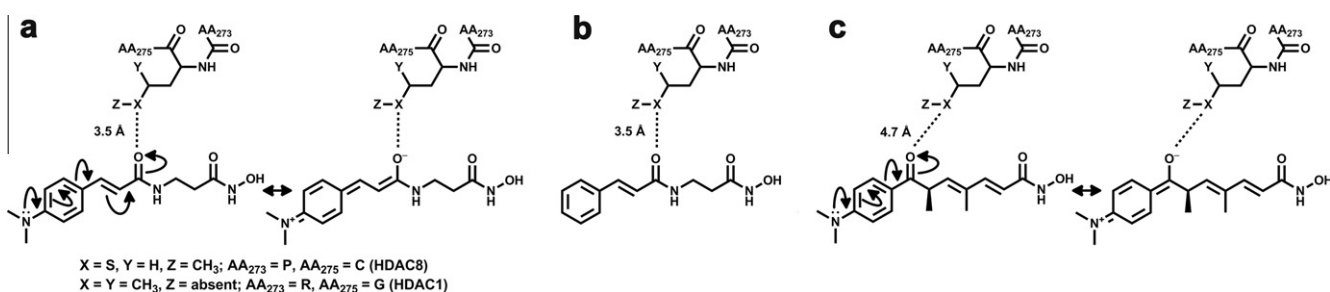


**Figure 4.** The ion-dipole repulsion between the negatively charged 5'-carbonyl oxygen atom of the zwitterionic resonance stabilized form of **2** and the sulfur atom of M274 (HDAC8) or the isobutyl group of Leu274 (HDAC1) (RHS, (a)) is posited to contribute to its limited potency as an HDAC1 inhibitor. Relative to **2**, the weaker dipole-dipole repulsion in **7** manifests as increased HDAC1 inhibitor potency (b). The distance between the 7'-carbonyl oxygen atom of **1**, which could exist in two resonance forms, and atoms of the corresponding side chains, is sufficient to prevent intermolecular repulsion (c).

## Acknowledgments

Funding to R. C. from the Cancer Institute NSW (08/RFG/1-12) and to T. L. from the National Health and Medical Research Council Australia (1006002) is kindly acknowledged.

## Supplementary data

Supplementary data associated with this article can be found, in the online version, at <http://dx.doi.org/10.1016/j.bmcl.2012.08.006>.

## References and notes

- Bolden, J. E.; Peart, M. J.; Johnstone, R. W. *Nat. Rev. Drug Discov.* **2006**, *5*, 769.
- Liu, T.; Kuljaca, S.; Tee, A.; Marshall, G. M. *Cancer Treat. Rev.* **2006**, *32*, 157.
- Bertrand, P. *Eur. J. Med. Chem.* **2010**, *45*, 2095.
- Marmion, C. J.; Griffith, D.; Nolan, K. B. *Eur. J. Inorg. Chem.* **2004**, 3003.
- Codd, R. *Coord. Chem. Rev.* **2008**, *252*, 1387.
- Richon, V. M.; Emiliani, S.; Verdin, E.; Webb, Y.; Breslow, R.; Rifkind, R. A.; Marks, P. A. *Proc. Natl. Acad. Sci. U.S.A.* **1998**, *95*, 3003.
- Codd, R.; Braich, N.; Liu, J.; Soe, C. Z.; Pakchung, A. A. H. *Int. J. Biochem. Cell Biol.* **2009**, *41*, 736.
- Ejje, N.; Lacey, E.; Codd, R. *RSC Adv.* **2012**, *2*, 333.
- Zhang, S.; Duan, W.; Wang, W. *Adv. Synth. Catal.* **2006**, *348*, 1228.
- Miller, T. A.; Witter, D. J.; Belvedere, S. *J. Med. Chem.* **2003**, *46*, 5097.
- Jung, M.; Brosch, G.; Kölle, D.; Scherf, H.; Gerhäuser, C.; Loidl, P. *J. Med. Chem.* **1999**, *42*, 4669.
- Whitehead, L.; Dobler, M. R.; Radetich, B.; Zhu, Y.; Atadja, P. W.; Claiborne, T.; Grob, J. E.; McRiner, A.; Pancost, M. R.; Patnaik, A.; Shao, W.; Shultz, M.; Tichkule, R.; Tommasi, R. A.; Vash, B.; Wang, P.; Stams, T. *Bioorg. Med. Chem. Lett.* **2011**, *19*, 4626.

13. HDAC1 assay. The HDAC1 Inhibitor Screening assay kit was purchased from Cayman Chemical Company. A FLUOstar Omega microplate reader was used at an excitation wavelength of 345 nm and an emission wavelength of 450 nm. Samples of **2–7** were prepared in methanol at five concentrations (10, 100, 250, 500, 1000  $\mu\text{M}$ ). Additional samples were prepared in methanol for **5** (25, 50, 75, 150, 200  $\mu\text{M}$ ) and **7** (1, 5, 25, 50  $\mu\text{M}$ ). The assay was conducted in triplicate in a 96-well microplate according to the instruction manual. The HDAC1 activity was completely inhibited with **1** at 1  $\mu\text{M}$ . The  $\text{IC}_{50}$  values of **2–7** were calculated using Prism software by fitting the data points with the equation:  $y = A - ((A \times x)/B + x)$ , where  $A = 100\%$  activity and  $B = \text{IC}_{50}$ . The inhibitory activity of **2–7** against other HDAC isoforms was not screened in this work.
14. Antiproliferative-activity. BE(2)-C neuroblastoma cells were treated with **2–7** at 50  $\mu\text{M}$  or with different dosages of TSA or SAHA. Seventy-two hours after treatment, relative numbers of cells were examined by the Alamar blue assay, measured as optical density (OD) units of absorbance, and expressed as a percentage of absorbance of the experimental samples over that of control samples (i.e., percentage change in cell number).
15. Marshall, G. M.; Liu, P. Y.; Gherardi, S.; Scarlett, C. J.; Bedalov, A.; Xu, N.; Iraci, N.; Valli, E.; Ling, D.; Thomas, W.; van Bekkum, M.; Sekyere, E.; Jankowski, K.; Trahair, T.; MacKenzie, K. L.; Haber, M.; Norris, M. D.; Biankin, A. V.; Perini, G.; Liu, T. *PLoS Genet.* **2011**, *7*, e1002135.
16. Suzuki, T.; Kouketsu, A.; Matsuura, A.; Kohara, A.; Ninomiya, S.-I.; Kohda, K.; Miyata, N. *Bioorg. Med. Chem. Lett.* **2004**, *14*, 3313.
17. Khan, N.; Jeffers, M.; Kumar, S.; Hackett, C.; Boldog, F.; Khramtsov, N.; Qian, X.; Mills, E.; Berghs, S. C.; Carey, N.; Finn, P. W.; Collins, L. S.; Tumber, A.; Ritchie, J. W.; Jensen, P. B.; Lichenstein, H. S.; Sehested, M. *Biochem. J.* **2008**, *409*, 581.
18. Watkins, C. J.; Romero-Martin, M.-R.; Moore, K. G.; Ritchie, J.; Finn, P. W.; Kalvinish, I.; Loza, E.; Starchenkov, I.; Dikovska, K.; Bokaldere, R. M.; Galite, V.; Vorona, M.; Andrianov, V.; Lolya, D.; Semenikhina, V.; Amolins, A.; Harris, C. J.; Duffy, J. E. S. **2002**, PCT Int. Appl. WO 2002026696.
19. Dowling, D. P.; Gantt, S. L.; Gattis, S. G.; Fierke, C. A.; Christianson, D. W. *Biochemistry* **2008**, *47*, 13554.
20. Schuetz, A.; Min, J.; Allali-Hassani, A.; Schapira, M.; Shuen, M.; Loppnau, P.; Mazitschek, R.; Kwiatkowski, N. P.; Lewis, T. A.; Maglathin, R. L.; McLean, T. H.; Bochkarev, A.; Plotnikov, A. N.; Vedadi, M.; Arrowsmith, C. H. J. *Biol. Chem.* **2008**, *283*, 11355.
21. Finnin, M. S.; Donigian, J. R.; Cohen, A.; Richon, V. M.; Rifkind, R. A.; Marks, P. A.; Breslow, R.; Pavletich, N. P. *Nature* **1999**, *401*, 188.
22. Bondi, A. *J. Phys. Chem.* **1964**, *68*, 441.
23. Coles, M.; Bicknell, W.; Watson, A. A.; Fairlie, D. P.; Craik, D. J. *Biochemistry* **1998**, *37*, 11064.
24. Tan, Z.; Shang, S.; Danishefsky, S. J. *Proc. Natl. Acad. Sci. U.S.A.* **2011**, *108*, 4297.
25. Somoza, J. R.; Skene, R. J.; Katz, B. A.; Mol, C.; Ho, J. D.; Jennings, A. J.; Luong, C.; Arvai, A.; Buggy, J. J.; Chi, E.; Tang, J.; Sang, B.-C.; Verner, E.; Wynands, R.; Leahy, E. M.; Dougan, D. R.; Snell, G.; Navre, M.; Knuth, M. W.; Swanson, R. V.; McRee, D. E.; Tari, L. W. *Structure* **2004**, *12*, 1325.